Langmuir

ARTICLE

pubs.acs.org/Langmuir

Using Microcontact Printing of Fibrinogen to Control Surface-Induced Platelet Adhesion and Activation

Lindsey E. Corum, Colin D. Eichinger, Tony W. Hsiao, and Vladimir Hlady*

Department of Bioengineering, University of Utah, 20 South 2030 East, Salt Lake City, Utah 84112, United States

ABSTRACT: The ability to promote or inhibit specific platelet−surface interactions in well-controlled environments is crucial to studying fundamental adhesion and activation mechanisms. Here, microcontact printing was used to immobilize human fibrinogen covalently in the form of randomly placed, micrometer-sized islands at an overall surface coverage of 20, 50, or 85%. The nonprinted background region was blocked with covalently immobilized human albumin. Platelet adhesion and morphology on each substrate were assessed using combined differential interference and fluorescence microscopy. At 20% coverage, most of the fibrinogen surface features were small round islands, and platelet adhesion and spreading areas were limited by the position and the size of the islands. Platelet circularity, indicated the morphology was mostly rounded. At 50% coverage, some fibrinogen islands coalesced and platelet adhesion and spreading areas increased. Platelet morphology was controlled by the shape of underlying fibrinogen islands, leading to more irregular spreading. At 85% coverage, the fibrinogen pattern was completely interconnected and both platelet adhesion and the spreading area were significantly higher than at lower coverage. In addition, platelets also spread over the albumin regions, suggesting that after a critical surface density of fibrinogen ligands is reached, platelet spreading is no longer inhibited by albumin. Increasing the overall fibrinogen coverage resulted in higher activation levels defined by key morphological characteristics of the spreading platelet.

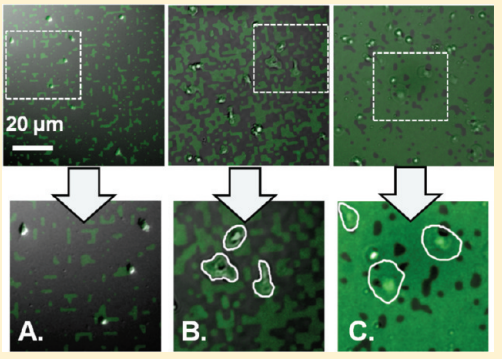

1. INTRODUCTION

Platelets are small anuclear cell fragments circulating in the bloodstream and play a critical role in clot formation when vascular injury occurs. At the site of injury, platelets become activated through specific interactions between protein agonists and membrane receptors.[1] Once activated, a host of responses occur, eventually leading to thrombus formation. Although clot formation at the site of vascular injury is critical to homeostasis, platelet activation can also occur on implanted vascular devices and continues to be a critical concern.[2−4] When a synthetic material first comes into contact with blood, plasma proteins capable of inducing platelet activation immediately adsorb to the surface.[4] The formation of thrombi on the surface of vascular devices can cause many complications and ultimately lead to its failure. In essence, the adsorbed protein layer, not the actual surface, determines the platelet response, thus an extensive amount of effort has been devoted to understanding both the nature of the adsorbed protein layer[5−8] and platelet−protein interactions.[9−12]

Platelet adhesion is supported by specific interactions between membrane receptors and exposed extracellular matrix or, in the case of vascular devices, adsorbed plasma proteins. The most abundant receptors on the platelet membrane, GPIb-V-IX and integrin $\alpha_{IIb}\beta_3$, interact with the plasma proteins' von Willibrand factor (vWf) and fibrinogen, respectively.[1,13,14] Specifically, GPIb-V-IX binds to surface-immobilized vWf to arrest platelets under flowing conditions. Although this interaction is weak and reversible, it is crucial in facilitating stable integrin $\alpha_{IIb}\beta_3$ fibrinogen binding, thus both proteins work synergistically to promote stable platelet adhesion.[15−17]

Following adhesion, platelet activation is characterized by morphological changes including filipod extension, lamellipod formation, and spreading as more specific adhesive contacts with adsorbed protein ligands are established. Activation also leads to the up-regulation of high-affinity binding sites for adhesion proteins involved in further platelet adhesion, activation, and aggregation.[18−20] Platelet spreading also facilitates the centralization of granules that secrete procoagulant factors involved in further platelet recruitment and activation.[18] An extensive amount of effort has been devoted to understanding both adhesion and activation; however, our understanding of many of these mechanisms is still incomplete. Although in vivo models provide the most accurate conditions for studying these mechanisms, it is difficult to elucidate cause−effect relationships because the biochemical events are often complex and highly interdependent. The ability to develop controlled in vitro studies where specific platelet−surface interactions are promoted or inhibited is crucial to improving our understanding of basic platelet mechanisms.

Microcontact printing has been demonstrated to be a powerful technique in many fundamental cell biology studies.[21,22] This tool is capable of generating well-defined patterns of immobilized protein ligands in which the type, size, shape, and

Received: March 21, 2011
Revised: April 22, 2011
Published: June 09, 2011

spacing are precisely controlled. Microcontact protein patterning has been used to study many different cell phenomena including adhesion, migration, apoptosis, and proliferation.[21,23−25] This technique has also been used to pattern 2-D protein arrays for high-throughput drug screening and disease diagnosis.[26]

Microcontact protein printing also has potential value in platelet adhesion and activation studies. Basabe-Desmonts et al. demonstrated that platelets could be isolated from whole blood using microcontact-printed dots of platelet-specific protein ligands. They were able to control overall adhesion by varying the size of the dots, demonstrating a potential application of microcontact protein printing in diagnostics for platelet functionality assays.[27] Ismagilov et al. recently used protein patterning to control a coagulation stimuli patch size and discovered that there exists a threshold initiation response.[28] However, despite these efforts, applications of microcontact printing to fundamental platelet adhesion studies are still relatively new. Variables including protein concentration, orientation, density, and conformation have all been hypothesized to affect the biomaterial-induced platelet response.[6,10,29,30] In many of these studies, protein substrates are prepared using adsorption to investigate these parameters, which does not allow control over the spatial distribution, ligand patch size, or surface ligand density, making the exact mechanisms difficult to elucidate.

In this work, random micrometer-sized fibrinogen patterns were covalently immobilized to reactive substrates using microcontact printing. Stamps with randomly patterned islands were generated at three surface coverage areas (20, 50, and 85%) and used for printing. Increasing the surface coverage area also increased the size of the fibrinogen islands as a result of the coalescence of randomly placed islands. Nonprinted regions of the substrate were passivated with covalently immobilized albumin. The effect of varying the average fibrinogen surface density, island size, and shape on platelet adhesion activation was observed and quantified using combined differential interference contrast (DIC), fluorescence, and scanning electron microscopy (SEM). Our goals were to investigate the extent to which the underlying fibrinogen pattern was able to control the platelet spreading morphology and to characterize the platelet response to substrates with variable fibrinogen ligand densities. It was found that both overall adhesion and activation could be controlled by varying the size of the immobilized fibrinogen islands. The platelet morphology was observed to be controlled by the shape of the underlying fibrinogen pattern. These studies have the potential to serve as a basis for further studies in which the adhesion response of morphological parameters can be correlated with physiological processes.

2. MATERIALS AND METHODS

2.1. Materials. Poly(dimethylsiloxane) (PDMS) stamps for microcontact protein printing were prepared from Sylgard 184 silicone elastomer (Dow Corning, Dublin, Ireland). Plasminogen-depleted human fibrinogen and albumin (essentially fatty acid-free) were from Calbiochem (Merck KGaA, Darmstadt, Germany) and Sigma-Aldrich (St. Louis, MO), respectively. Nexterion-H reactive microscope slides (Schott, Elmsford, NY) were used for protein covalent immobilization. Alexa Fluor 488 succinimidyl ester fluorophore (Invitrogen, Carlsbrad, CA) was used for fibrinogen labeling. Labeled fibrinogen was isolated using PD-10 columns (GE Healthcare, Waukesha, WI). Any labeled protein aggregates were removed using 0.22 μm low-protein-binding PES syringe filters (Millipore, Billerica, MA). Silicon cantilevers

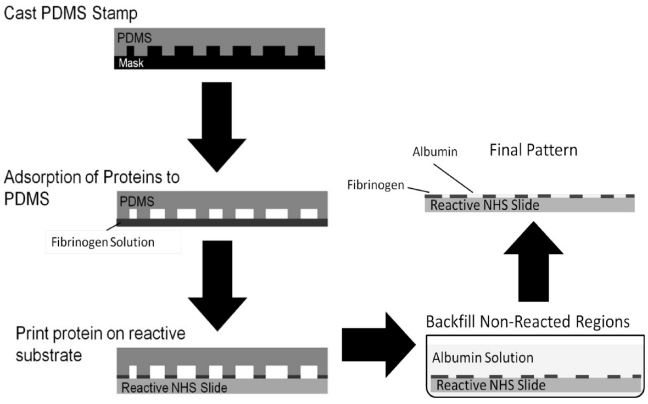

Figure 1. Schematic of the microcontact protein printing process leading to the covalent immobilization of fibrinogen and albumin.

(Mikromasch, San Jose, CA) were used for lateral force microscopy measurements. Prostaglandin E1, used to prevent premature activation during platelet preparation, was from Sigma-Aldrich (St. Louis, MO).

2.1.1. Buffers. A protein printing buffer was prepared with 150 mM sodium phosphate and 0.01% sarkosyl or Tween 20 (pH 8.5). A sodium bicarbonate buffer was prepared with 0.1 M NaH_2CO_3, and the pH was adjusted to 8.5. The Tyrodes-HEPES buffer was prepared with 134 mM NaCl, 12 mM $NaHCO_3$, 2.9 mM KCl, 0.34 mM Na_2HPO_4, 1 mM $MgCl_2$, and 10 mM HEPES. Glucose (5 mM) and bovine albumin (0.3 g) were added to the buffer the day of use, and the pH was adjusted to 7.4. Phosphate-buffered saline (PBS) was prepared with 137 mM NaCl, 2.7 mM KCl, 4.3 mM Na_2HPO_4, and 1.47 mM KH_2PO_4, and the pH was adjusted to 7.4.

2.2. Methods. *2.2.1. Preparation of PDMS Stamps.* To produce PDMS stamps, Mathematica (Wolfram, Champaign, IL) was used to produce patterns of randomly distributed pixels with 85, 50, and 20% surface coverage areas. These patterns were used as a template to fabricate masks with micrometer-sized features (total mask area = 1 cm^2) using standard photolithography techniques. Sylgard 184 silicone elastomer was mixed with curing agent in a 10:1 ratio and poured over the patterned mask. PDMS was degassed by placing the samples under vacuum for 30 min. The samples were cured for 30 min at 100 °C and carefully peeled away from the patterned mask. This was followed by an additional curing step for 60 min at 30 °C.

2.2.2. Printing Covalently Immobilized Fibrinogen Patterns. PDMS stamps were "inked" with fibrinogen in the protein printing buffer (c = 1 mg/mL) for 15 min, rinsed in Milli-Q water, and dried with N_2 gas. The fibrinogen-covered stamps were placed in contact with Nexterion-H reactive slides for 45 min, allowing for protein covalent immobilization (Figure 1). These slides contain a coating in which a cross-linked poly(ethylene glycol) (PEG) layer is functionalized with *N*-hydroxysuccinimide (NHS) esters, providing a means for covalent immobilization through the protein amine groups.[31] After fibrinogen was printed, the nonstamped regions were passivated by incubating the samples in an albumin solution in protein printing buffer (c = 1 mg/mL) for 30 min. Following protein immobilization, samples were vigorously rinsed in 1% Tween to remove any protein not covalently attached to the surface. Samples were then rinsed thoroughly with Milli-Q water, dried with N_2 gas, and stored under vacuum until use.

2.2.3. Fibrinogen Labeling. To visualize immobilized protein patterns, fibrinogen was labeled with Alexa Fluor 488 succinimidyl ester (Invitrogen). Human fibrinogen (c = 10 mg/mL, Calbiochem) in 0.1 M sodium bicarbonate buffer (pH 8.5) was incubated for 2 h with Alexa Fluor 488 (c = 0.25 mg/mL). After incubation, the protein solution was loaded into PD-10 Sephadex columns (GE Healthcare) to separate labeled fibrinogen from nonreacted fluorophores. Labeled protein was eluted with

protein printing buffer (pH 8.5). Protein aggregates were filtered out using 0.22 μm low-protein-binding PES syringe filters (Millipore), and the labeled protein was immediately frozen at −20 °C until use.

2.2.4. Surface Characterization. Lateral force microscopy (LFM) was used to characterize the printed fibrinogen samples. Measurements were obtained in air using an Explorer AFM (TopoMetrix, Santa Clara, CA) with silicon cantilevers (nominal force constant 0.03 N/m, radius of tip curvature <10 nm). The lateral force was recorded on a sample area of 50 × 50 μm^2 for each fibrinogen pattern (n = 10), and ImageJ (W. Rasband, NIH) was used to quantify the area and size of the fibrinogen surface features. The integrity of the fibrinogen patterns was also confirmed using fluorescence microscopy by printing Alexa Fluor-488 (Invitrogen)-labeled fibrinogen as previously described.

2.2.5. Platelet Adhesion Studies. Fresh whole blood was collected from healthy human donors in a 1:7 acid citrate/dextrose solution. Washed platelets were prepared by first centrifuging the whole blood for 15 min at 1500 rpm to separate platelet-rich plasma (PRP). The PRP supernatant was aspirated using a transfer pipet. Prostaglandin E_1 (c = 300 nM) was added to the PRP to inhibit aggregation during preparation.[32] PRP was then centrifuged for another 15 min at 2100 rpm to isolate the platelet pellet. The platelet-poor plasma (PPP) supernatant was carefully discarded, and the platelet pellet was gently resuspended in prewarmed Tyrode's HEPES buffer (37 °C, pH 7.4).[33] Platelets were counted using a hemocytometer, and the concentration was diluted to 1.0 × 10^7 platelets/mL. The washed platelet suspension was maintained at 37 °C prior to each experiment. Each sample was incubated in the washed platelet suspension for 5 min and rinsed twice with PBS to remove unbound platelets. Samples were fixed with 3.2% gluteraldehyde (t = 30 min) and rinsed three times with PBS. To characterize the platelet response, the adhesion, spreading area, and circularity were quantified for each sample. Adhered platelets were visualized using a DIC microscope (Nikon Diaphot 300, 60× LWD, NA 0.9). Overall adhesion was quantified by measuring the number of adhered platelets for each fibrinogen coverage (n = 30). The spreading area and circularity, defined as perimeter^2/{4π(area)}, were calculated by measuring the average area and perimeter for platelets (n = 100) on five different samples for each fibrinogen coverage. For each data set, a 95% confidence was calculated from the standard error of the mean, and the statistical significance was calculated using an unpaired t test.

2.2.6. SEM Morphological Analysis. Fixed platelet samples were dehydrated by incubating in ascending ethanol (50, 75, and 100%) solutions for 15 min each. Samples were dried and sputter coated with a 10 nm layer of gold with a Cressington 108 auto sputter coater. SEM images were obtained using a Hitachi S-3000N SEM at 20 kV.

3. RESULTS

3.1. Characterization of Immobilized Fibrinogen Patterns. Microcontact protein printing was used to immobilize micrometer-sized human fibrinogen islands covalently on Nexterion-H slides at a relative surface coverage of 20, 50, or 85%. The integrity of the surface, the size of the fibrinogen islands, and the printing efficiency were characterized using both fluorescence and LFM. Samples were vigorously rinsed in a 1% Tween surfactant solution to remove nonspecifically immobilized protein. Alexa Fluor 488-labeled fibrinogen surface patterns were visualized after surfactant treatment, suggesting that the protein was covalently immobilized (Figure 2A). Examining fibrinogen surface patterns by fluorescence microscopy was also used to assess the integrity of the fibrinogen patterns and ensure that no defects were present prior to conducting experiments.

LFM was used to characterize the average protein feature size and the printing efficiency of the PDMS stamps at each fibrinogen coverage (Figure 2B). LFM images showed good contrast between the printed fibrinogen and nonprinted albumin regions. The actual coverage of printed fibrinogen was quantified for each sample (n = 10) and compared with target values (Table 1). No significant difference between actual and target values was found, confirming the fidelity of protein transfer. The mean fibrinogen island size on 20% coverage samples was 5.3 ± 0.4 μm^2. The background albumin pattern was completely interconnected, thus calculating an average size was not possible. At 50%, the average fibrinogen and albumin feature sizes were 84.1 ± 31.4 and 68.2 ± 34.0 μm^2, respectively. A large standard deviation was observed, suggesting a heterogeneous distribution of island sizes on these samples. At 85%, the printed fibrinogen features were completely interconnected. The mean albumin island size was 4.8 ± 0.6 μm^2.

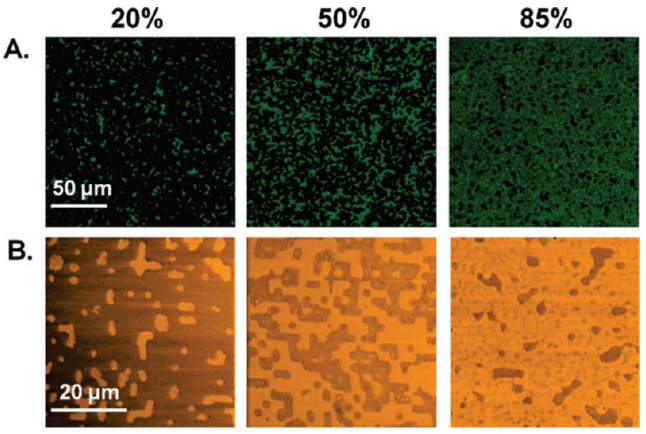

Figure 2. (A) Representative fluorescence (green = Alexa Fluor 488-labeled fibrinogen) and (B) lateral force AFM images (orange = fibrinogen islands) of 20, 50, and 85% relative surface coverages of printed fibrinogen.

Table 1. Printing Efficiency and Average Protein Island Size for Printed Patterns (n = 10)

target coverage	actual coverage (%)	size of fibrinogen islands (μm^2)	size of albumin islands (μm^2)
20%	21.1 ± 1.1	5.3 ± 0.4	N/A
50%	51.6 ± 2.0	84.1 ± 31.4	68.2 ± 34.0
85%	85.5 ± 0.9	N/A	4.8 ± 0.6

3.2. Platelet Adhesion and Spreading on Well-Defined Fibrinogen Patterns. The effect of the underlying fibrinogen pattern on platelet adhesion and spreading was studied by printing randomly placed micrometer-sized fibrinogen islands at different relative surface coverage areas (20, 50, or 85%). Because of the random nature of island placement, each coverage area corresponded to a different population of printed islands, thus correlations could be made on the basis of the size and shape of the stimuli presented to platelets. On each substrate, Alexa Fluor 488-labeled fibrinogen patterns were observed using fluorescence microscopy (Figure 3, row 1) and the adhered platelets were observed using DIC microscopy (Figure 3, row 2). Corresponding images were superimposed to study the spatial registration between the platelets and the underlying protein features (Figure 3, row 3). At 20% fibrinogen coverage, almost no spreading was observed (Figure 3A). The size of the platelets was small and their shape was rounded, and in the case when platelets

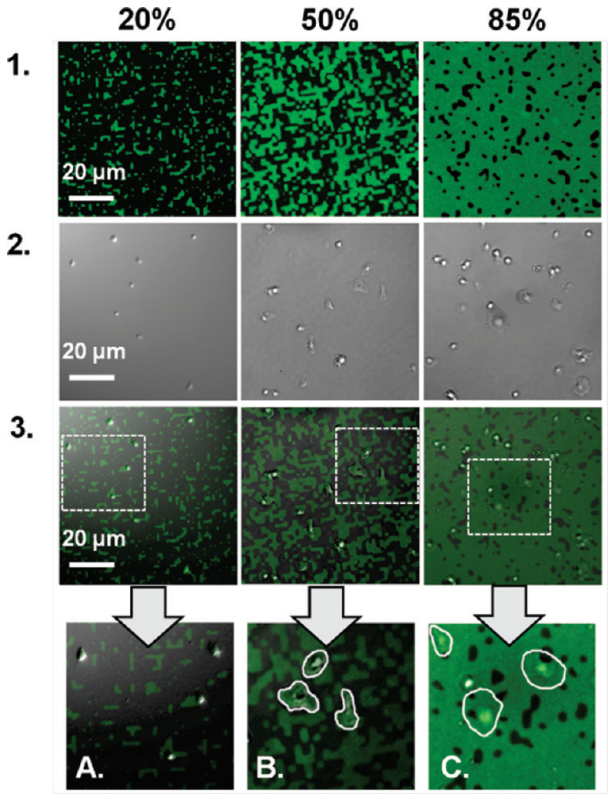

Figure 3. Platelet adhesion to covalently immobilized fibrinogen patterns at coverages of 20, 50, and 85%. The nonprinted region is blocked with covalently immobilized albumin. The top and middle rows contain fluorescent images of fibrinogen patterns and DIC images of platelet adhesion and spreading, respectively. (A) The bottom row includes superimposed images, where at 20% platelets rarely spread and when they do their size is strictly limited by the size of the underlying fibrinogen pattern. (B) At 50%, platelets are able to spread, but their morphology almost strictly depends on the shape of the underlying fibrinogen pattern. (C) At 85%, platelets are able to spread over inert albumin regions, and the morphology is not necessarily dependent on the underlying fibrinogen pattern.

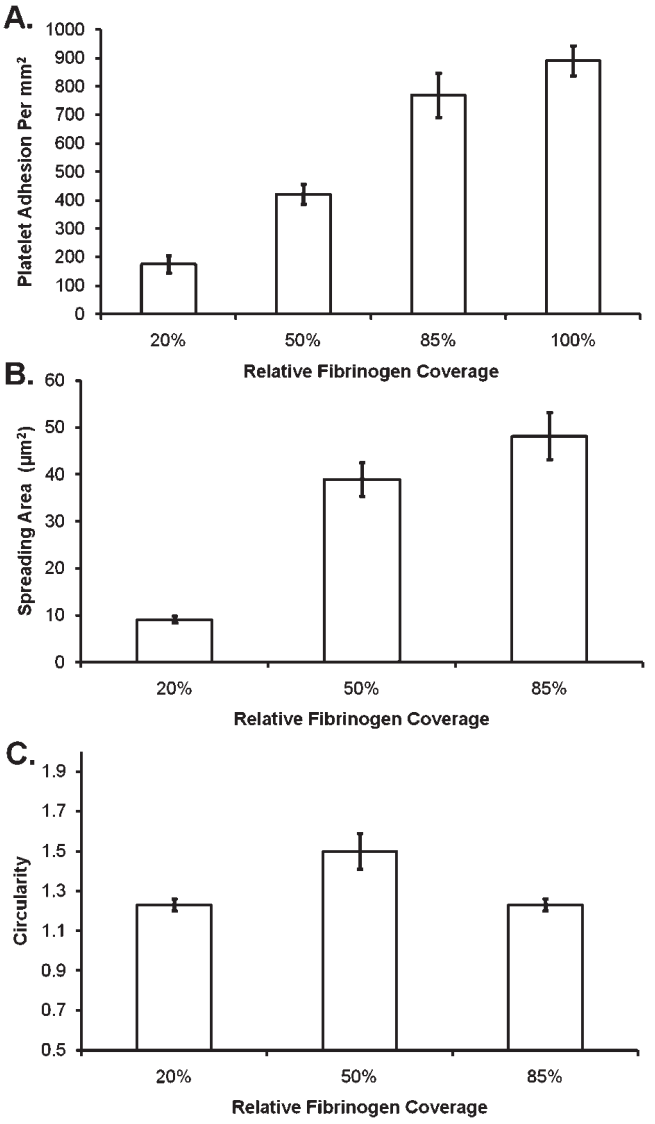

Figure 4. (A) Platelet adhesion to printed fibrinogen substrates at 20, 50, 85, and 100% relative surface coverage ($n = 30$). A Nexterion-H slide covered with albumin showed negligible platelet adhesion (data not shown). (B) Average platelet spreading area on samples with each relative fibrinogen coverage ($n = 100$). (C) Average platelet circularity for each relative fibrinogen coverage ($n = 100$). All error bars represent the standard error of the mean with a 95% confidence interval.

did spread, their morphology was strictly limited by the size of the underlying fibrinogen islands. At 50% fibrinogen coverage, more extensive platelet spreading was observed; however, the morphology was still dependent on the shape of the underlying pattern (Figure 3B). At 85% coverage, fibrinogen islands coalesced into a continuous interconnected pattern and extensive spreading was observed. In most cases, platelets spread over the albumin islands as well (Figure 3C).

3.3. Quantifying the Effect of Relative Fibrinogen Surface Coverage on the Platelet Response. To quantify the platelet response, the adhesion, spreading area, and circularity were measured for each fibrinogen coverage area (20, 50, and 85%). Average adhesion was calculated for each sample (Figure 4A, $n = 30$). Values were compared with a 100% fibrinogen substrate prepared by printing a flat PDMS stamp. Platelet adhesion to the albumin background was also measured but was found to be negligible (data not shown). The overall adhesion increased with increasing fibrinogen surface coverage, demonstrating that random island printing can be used as a means to titrate the adhesion response.

The average platelet spreading area is shown in Figure 4B. The average spreading area increased with increasing fibrinogen surface coverage (i.e., with increased size of the underlying fibrinogen islands). At 20% relative fibrinogen coverage, almost no spreading was observed and the average area per platelet was $9.1 \pm 0.7\ \mu m^2$. Compared with the average fibrinogen feature size of $5.3 \pm 0.4\ \mu m^2$ (Table 1), it appeared that the platelets formed a stable adhesion only on larger fibrinogen islands. The platelet spreading area increased with increasing fibrinogen surface coverage to 50%, equaling $38.9 \pm 3.6\ \mu m^2$, an area that was less than half of the average size of the coalesced fibrinogen features (Table 1). For this fibrinogen surface coverage, the shape of the platelets was strongly affected by the shape of fibrinogen islands (Figure 3B). At 85% fibrinogen coverage, the spreading area was $48.2 \pm 5.0\ \mu m^2$. The increase in the platelet spreading area between 20 and 50% was much more

dx.doi.org/10.1021/la201064d |*Langmuir* 2011, 27, 8316–8322

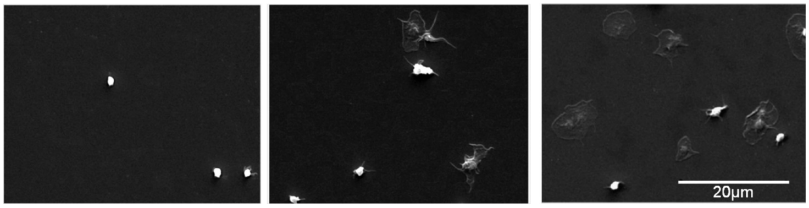

Figure 5. Scanning electron micrograph images of platelets spreading on surfaces printed at (A) 20, (B) 50, and (C) 85% relative fibrinogen coverage (scale bar = 20 μm).

Table 2. Qualitative Assessment of Platelet Activation Based on the Morphology of Adherent Platelets (n = 10)

	stage 1: adherent platelets	stage 2: partially activated (I)	stage 3: partially activated (II)	stage 4: fully activated
relative fibrinogen coverage (%)	platelets adhere and maintain a small spherical morphology (%)	initiation of filopodium formation and extension (%)	extensive filopodium formation and the beginning of spreading (%)	filopodium retraction, platelet displays a round, flat morphology (%)
20	37.0 ± 8	63.0 ± 8	0	0
50	2.5 ± 2.1	21.7 ± 4.9	63.1 ± 4.5	12.7 ± 2.4
85	0.4 ± 0.7	17.6 ± 3.6	59.0 ± 4.3	23.0 ± 3.5

drastic than between 50 and 85%, though all were significantly different ($p < 0.001$).

Circularity has been recognized as a way to quantify the platelet morphological response.[34,35] Upon activation, the circularity will approach 1 as platelets reach their fully spread morphology.[35] To determine the extent to which spreading was affected by the underlying fibrinogen pattern, circularity was calculated (n = 100) for each sample. If circularity is greater than 1, the platelet shape is irregular, with higher values corresponding to shapes that were less circular. At 20 and 85% relative fibrinogen coverage, there was no significant difference in circularity (Figure 4C). This is not surprising because although there was a significant difference in spreading area, both adhered and fully spread platelets display circular morphologies. At 50% relative fibrinogen coverage, a significant ($p < 0.001$) increase in circularity was observed. This was due to the shape of the underlying fibrinogen pattern supporting only irregular morphologies, not allowing the platelets to spread fully (also seen in Figure 3B).

3.4. Assessment of Platelet Morphological Parameters. To investigate further the effect of varying fibrinogen feature sizes on platelet morphology, high-resolution SEM images were taken for each sample. At 20% fibrinogen coverage (Figure 5A), almost no spreading occurred and platelets displayed small spherical morphology. In some cases, however, platelet filopodia were observed, suggesting that these adhesion events still resulted in activation and may support platelet recruitment and aggregation over time. Samples with 50% fibrinogen coverage (Figure 5B) exhibited more extensive spreading and filopodium formation, but the morphologies were irregular in shape. As discussed above, this is the result of the underlying pattern restricting platelet spreading to regions in which immobilized fibrinogen is present (Figure 3B). At 85% coverage (Figure 5C), extensive spreading occurred and more platelets were observed to be in a fully spread circular shape.

Because platelet activation and morphology are interrelated, the platelet shape change was qualitatively assessed by examining the extent of filopodium formation and spreading on each sample (Table 2). Platelet activation levels were divided into four stages: (1) adherent but not spread, (2) initial formation of filopodia, (3) extensive filopodium formation and beginning of spreading, and (4) filopodium retraction and flat, rounded morphologies. SEM images (n = 10) for each relative fibrinogen coverage were examined. The number of platelets in each category was calculated and normalized by the total number of adhered platelets. These values were then averaged to give an overall mean percent and standard error for each sample. The number of platelets that adhered but were not activated and the number of platelets that showed initial stages of filopodium formation decreased with increasing fibrinogen feature size. The number of platelets that showed extensive filopodium formation or rounded flat morphologies increased at higher fibrinogen area fractions. In fact, at 20% coverage, no platelets in the third or fourth stages of activation were observed. These results all suggest that overall platelet activation can be controlled by varying the size of the fibrinogen islands.

4. DISCUSSION

In this study, microcontact printing was used to characterize the platelet response to covalently immobilized fibrinogen patterns with varying surface coverage areas. Fibrinogen was selected as the model ligand for these studies because of its multiple roles in platelet adhesion, activation, and aggregation.[11,36] Microcontact printing was chosen as the patterning technique because it has been proven to generate well-defined ligand patterns reproducibly in other cellular applications.[21] The surface density of immobilized fibrinogen was controlled by varying the size and number of random microfeatures on PDMS stamps. The use of randomized patterns was chosen over more traditionally used dotted patterns because they are more relevant to the random adsorption of proteins to the biomaterial interface under physiological conditions. Covalent immobilization of the fibrinogen ligands on NHS reactive substrates maintained the integrity and stability of the patterns, ensuring no desorption or leaching of immobilized protein over time. Furthermore, the test samples were coated with a thin PEG-based hydrogel modified with terminal NHS ester groups and show a minimal tendency toward nonspecific protein adsorption and low platelet adhesion.[37] In addition, after fibrinogen immobilization, the non printed

regions were passivated with covalently immobilized albumin, a plasma protein known to be relatively inert to platelets.[38] The use of diluted washed platelet suspensions was chosen to control the surface protein content and ensure that the phenomena observed were solely due to platelet−fibrinogen interactions. In this study, the use of whole blood would have been inappropriate. The use of washed platelets avoids the complexity of whole blood interactions where protein exchange, platelet recruitment, and aggregation and inflammatory responses may have all occurred at the same time, making cause−effect relationships impossible to elucidate. The washed platelet concentration was optimized to 10^7 platelets/mL to minimize aggregation and ensure that the observed platelet response was due to platelet−surface and not platelet−platelet interactions.

In Figure 3A−C, we observed that platelet adhesion and morphology both depended on the size and density of the underlying fibrinogen features. This was further confirmed by quantifying the overall adhesion, spreading area, and circularity in Figure 4A−C. Specifically, at 50% surface coverage we observed that platelet spreading was strictly limited to the underlying fibrinogen pattern (Figure 3B) and that circularity values suggested more irregular morphologies (Figure 4C). At 85% surface coverage, platelet spreading no longer strictly adhered to the underlying fibrinogen pattern (Figure 3C) and circularity values suggested more rounded morphologies (Figure 4C). This may be due to the full interconnectivity of fibrinogen patterns at this level of surface coverage. Once platelets adhered, a path around the small inert albumin islands was available to facilitate spreading. Also, it may be possible that there exists a threshold ligand density and/or spacing necessary to facilitate platelet adhesion and spreading. Interactions between fibrinogen and integrin $\alpha_{IIb}\beta_3$ receptors on the platelet membrane are critical in signaling cytoskeletal reorganizational events,[39] thus it is likely that the potential number of ligand−receptor interactions is important in determining the platelet response.

It has been postulated that the fibrinogen ligand density is a crucial parameter in biomaterial-induced platelet adhesion and activation;[6,29,34] however, to date, surface density has been controlled by varying the bulk concentration of the fibrinogen solution used to preadsorb the test samples. It is well known that biomaterial-induced fibrinogen−platelet interactions are mediated by the conformational exposure of binding epitopes upon adsorption.[9,10] It is also known that at very high bulk protein concentrations the protein adsorbs to the surface at a much faster rate, limiting the ability of the protein to unfold because of tight packing of the adsorbed protein.[40] Taken together, it is impossible to elucidate whether the changes in the platelet response are due to the density of the fibrinogen molecules or the ability of fibrinogen to unfold at lower bulk concentrations in these adsorption studies. Microcontact printing presents a method to control the placement and density of fibrinogen ligands precisely, allowing for a direct correlation to be made. Our studies actually indicate that there may be a threshold density or coverage area that will support normal platelet spreading/activation and eliminate the uncertainty that arises when protein test samples are prepared by simple adsorption.

Platelet shape change facilitates activation mechanisms crucial in ensuring the proper hemostatic response. Spreading induces $\alpha_{IIb}\beta_3$ activation and cytoskeletal reorganization events that lead to platelet degranulation and amplification of the coagulation response.[39,41,42] Filopodium formation facilitates platelet−fibrinogen interactions and aggregation, and lamellipodium formation is crucial in arresting vascular leakage upon vessel injury.[42,43] In vitro vascular injury models are commonly used to understand fundamental coagulation mechanisms. Specifically, the platelet response and thrombus formation have been investigated on surfaces preadsorbed with agonists such as collagen, fibrinogen, and vWf.[44−46] It has been demonstrated that both fibrinogen and vWf are capable of mediating platelet adhesion and aggregate formation through synergistic interactions between integrin $\alpha_{IIb}\beta_3$ and GPIb-X-IV.[17,47] The ability to control the type and size of platelet-activating ligand patches can be used to correlate the morphological parameters with physiological events such as exposure of a small lesion in the vascular endothelial layer to circulating blood. The lesion size determines the number of ligands available for platelet activation and subsequently the stimuli requirements for receptor expression/distribution, intracellular calcium changes, and the secretion of platelet recruiting agents. Thus, the techniques described here could be applied to physiologically relevant binary protein models, for example, collagen-vWf or fibrinogen-vWf, and could be used to study the mechanisms involved in these processes.

Morphology has been demonstrated to be an important variable in controlling many different cellular events.[23,24,48] For example, Chen et al. used the microcontact printing of extracellular matrix ligands to restrict endothelial cell spreading that resulted in an increase in apoptosis.[47] Cytoskeletal reorganization events have also been implicated in many platelet-activation mechanisms;[18,39,42] however, the use of micropatterned substrates to control platelet spreading has not been explored. Here, the underlying fibrinogen ligand feature size and density were shown to control key platelet morphological characteristics associated with surface-induced platelet activation as characterized quantitatively (Figure 4B,C) and qualitatively (Figure 5 and Table 2).

Given that platelet spreading is mediated by integrin−protein interactions, Grunkemeier et al. explored the role of different protein ligands in spreading mechanisms. Specifically, they investigated possible synergistic platelet shape change mechanisms by comparing spreading on polystyrene surfaces preadsorbed with a binary vWf-Fbg mixture with homogeneous controls. More spreading was observed on the binary protein surface, suggesting a synergistic role in platelet spreading; however, because protein was adsorbed, specific local protein−platelet effects could not be visualized.[49] The techniques presented here will facilitate future studies investigating these mechanisms with precise control of the type, size, and position of the surface-immobilized protein features.

5. CONCLUSIONS

This study demonstrated that the surface-induced platelet response could be controlled by the size and shape of immobilized protein ligands. Specifically, microcontact printing was used to produce randomly placed, covalently immobilized, micrometer-sized fibrinogen islands over three different surface coverage areas as characterized by fluorescence and lateral force microscopy. It was found that the fibrinogen island density, size, and shape affected both adhesion and morphological changes and that these effects could be titrated by varying the overall fibrinogen coverage. The ubiquitous nature of the immobilization procedure allows the same technique to be applied to any protein of interest and may serve to study local platelet−ligand interactions further. Although in vivo models provide the most

accurate conditions for studying these mechanisms, it is difficult to elucidate cause−effect relationships because the biochemical events are often complex and highly interdependent. The ability to develop controlled in vitro studies where specific platelet−surface interactions are promoted or inhibited is crucial to improving our understanding of basic platelet mechanisms.

AUTHOR INFORMATION

Corresponding Author

*E-mail: vladimir.hlady@utah.edu.

ACKNOWLEDGMENT

This work was supported by the National Institutes of Health (5RO1 HL84586) and the American Heart Association (10PRE4010047). We thank Dr. Andy Weyrich and his group for generously providing human blood for our studies and Mr. Caleb Campbell for his assistance with data analysis.

REFERENCES

(1) Ruggeri, Z. M.; Mendolicchio, G. L. *Circ. Res.* **2007**, *100*, 1673–1685.
(2) Gorbet, M. B.; Sefton, M. V. *Biomaterials* **2004**, *25*, 5681–5703.
(3) Ratner, B. D. *Biomaterials* **2007**, *28*, 5144–5147.
(4) Andrade, J. D.; Hlady, V. *Adv. Polym. Sci.* **1986**, *79*, 1–63.
(5) Malmsten, M. *J. Colloid Interface Sci.* **1998**, *207*, 186–199.
(6) Moskowitz, K. A.; Kudryk, B.; Coller, B. S. *Thromb. Haemost.* **1998**, *79*, 824–831.
(7) Sivaraman, B.; Fears, K. P.; Latour, R. A. *Langmuir* **2009**, *25*, 3050–3056.
(8) Xu, L. C.; Siedlecki, C. A. *Langmuir* **2009**, *25*, 3675–3681.
(9) Wu, Y.; Simonovsky, F. I.; Ratner, B. D.; Horbett, T. A. *J. Biomed. Mater. Res.* **2005**, *74A*, 722–738.
(10) Sivaraman, B.; Latour, R. A. *Biomaterials* **2010**, *31*, 832–839.
(11) Tsai, W.; Grunkemeier, J. M.; McFarland, C. D.; Horbett, T. A. *J. Biomed. Mater. Res.* **2002**, *60*, 348–359.
(12) Corum, L. E.; Hlady, V. *Biomaterials* **2010**, *12*, 3148–3155.
(13) Marguerie, G. A.; Plow, E. F.; Edgington, T. S. *J. Biol. Chem.* **1979**, *254*, 5357–5363.
(14) Andrews, R. K.; Gardiner, E. E.; Shen, Y.; Whisstock, J. C.; Berndt, M. C. *Int. J. Biochem. Cell Biol.* **2003**, *35*, 1170–1174.
(15) Kwak, D.; Wu, Y.; Horbett, T. A. *J. Biomed. Mater. Res.* **2005**, *74A*, 69–83.
(16) Nesbitt, W. S.; Kulkarni, S.; Giuliano, S.; Goncalves, I.; Dopheide, S. M.; Yap, C. L.; Harper, I. S.; Salem, H. H.; Jackson, S. P. *J. Biol. Chem.* **2002**, *277*, 2965–2972.
(17) Savage, B.; Saldívar, E.; Ruggeri, Z. M. *Cell* **1996**, *84*, 289–297.
(18) Hartwig, J. H. *J. Cell Biol.* **1992**, *118*, 1421–1442.
(19) Shattil, S. J.; Ginsberg, M. H.; Brugge, J. S. *Curr. Opin. Cell Biol.* **1994**, *6*, 695–704.
(20) Goncalves, I.; Hughan, S. C.; Schoenwaelder, S. M.; Yap, C. L.; Yuan, Y.; Jackson, S. P. *J. Biol. Chem.* **2003**, *278*, 34812–34822.
(21) Kane, R. S.; Takayama, S.; Ostuni, E.; Ingber, D. E.; Whitesides, G. M. *Biomaterials* **1999**, *20*, 2363–2376.
(22) Xia, Y.; Whitesides, G. M. *Annu. Rev. Mater. Sci.* **1998**, *28*, 153–184.
(23) Dike, L. E.; Chen, C. S.; Mrksich, M.; Tien, J.; Whitesides, G. M.; Ingber, D. E. *In Vitro Cell. Dev. Biol.: Anim.* **1999**, *35*, 441–448.
(24) Singhvi, R.; Kumar, A.; Lopez, G. P.; Stephanopoulos, G. N.; Wang, D. I.; Whitesides, G. M.; Ingber, D. E. *Science* **1994**, *264*, 696–698.
(25) Chen, C. S.; Mrksich, M.; Huang, S.; Whitesides, G. M.; Ingber, D. E. *Science* **1997**, *276*, 1425–1428.
(26) Lin, S. C.; Tseng, F. G.; Huang, H. M.; Huang, C. Y.; Chieng, C. C. *Fresenius' J. Anal. Chem.* **2001**, *371*, 202–208.
(27) Basabe-Desmonts, L.; Ramstrom, S.; Meade, G.; O'Neill, S.; Riaz, A.; Lee, L. P.; Ricco, A. J.; Kenny, D. *Langmuir* **2010**, *26*, 14700–14706.
(28) Kastrup, C. J.; Shen, F.; Runyon, M. K.; Ismagilov, R. F. *Biophys. J.* **2007**, *93*, 2969–2977.
(29) Jiroušková, M.; Jaiswal, J. K.; Coller, B. S. *Blood* **2007**, *109*, 5260–5269.
(30) Tsai, W.; Grunkemeier, J. M.; Horbett, T. A. *J. Biomed. Mater. Res.* **1999**, *44*, 130–139.
(31) Takahashi, H.; Emoto, K.; Dubey, M.; Castner, D. G.; Grainger, D. W. *Adv. Funct. Mater.* **2008**, *18*, 2079–2088.
(32) Mustard, J. F.; Packham, M. A. *Pharm. Rev.* **1970**, *22*, 97–187.
(33) Watson, S. P.; Authi, K. S. *Platelets: A Practical Approach*; Oxford University Press: Oxford, U.K., 2002; Chapter 1.
(34) Massa, T. M.; Yang, M. L.; Ho, J. Y.; Brash, J. L.; Santerre, J. P. *Biomaterials* **2005**, *26*, 7367–7376.
(35) Park, K.; Mao, F.; Park, H. *Biomaterials* **1990**, *11*, 24–31.
(36) Grunkemeier, J. M.; Tsai, W. B.; Mcfarland, C. D.; Horbett, T. A. *Biomaterials* **2000**, *21*, 2243–2252.
(37) Harbers, G. M.; Emoto, K.; Greef, C.; Metzger, S. W.; Woodward, H. N.; Mascali, J. J.; Grainger, D. W.; Lochhead, M. J. *Chem. Mater.* **2007**, *19*, 4405–4414.
(38) Amiji, M.; Park, H.; Park, K. *J. Biomater. Sci., Polym. Ed.* **1992**, *3*, 375–388.
(39) Haimovich, B.; Lipfert, L.; Brugge, J. S.; Shattil, S. J. *J. Biol. Chem.* **1993**, *268*, 15868–15877.
(40) Nakanishi, K.; Sakiyama, T.; Imamura, K. *J. Biosci. Bioeng.* **2001**, *91*, 233–244.
(41) Flaumenhaft, R.; Dilks, J. R.; Rozenvayn, N.; Monahan-Earley, R. A.; Feng, D.; Dvorak, A. M. *Blood* **2005**, *105*, 3879–3887.
(42) Fox, J. E.; Phillips, D. R. *J. Biol. Chem.* **1982**, *257*, 4120–4126.
(43) Cramer, E. M.; Fontenay, M. *Hemostasis and Thrombosis: Basic Principles and Clinical Practice*, 5th ed.; Lippincott Williams & Wilkins: Philadelphia, 2006.
(44) Zaidi, T. N.; McIntire, L. V.; Farrell, D. H.; Thiagarajan, P. *Blood* **1996**, *88*, 2967–2972.
(45) Neeves, K. B.; Maloney, S. F.; Fong, K. P.; Schmaier, A. A.; Kahn, M. L.; Brass, L. F.; Diamond, S. L. *J. Thromb. Haemost.* **2008**, *6*, 2193–2201.
(46) Colace, T.; Falls, E.; Zheng, X. L.; Diamond, S. L. *Ann. Biomed. Eng.* **2011**, *39*, 922–929.
(47) Savage, B.; Shattil, S. J.; Ruggeri, Z. M. *J. Biol. Chem.* **1992**, *267*, 11300–11306.
(48) Chen, C. S.; Mrksich, M.; Huang, S.; Whitesides, G. M.; Ingber, D. E. *Biotechnol. Prog.* **1998**, *14*, 356–363.
(49) Grunkemeier, J. M.; Tsai, W. B.; Horbett, T. A. *J. Biomater. Sci., Polym. Ed.* **2001**, *12*, 1–20.